Journal of Applied Biology & Biotechnology Vol. 12(6), pp. 208-217, Nov-Dec, 2024
Available online at http://www.jabonline.in
DOI: 10.7324/JABB.2024.175264

Anticancer effect of bioactive compound Apparicine isolated from the *Tabernaemontana divaricata* on retinoblastoma cancer cell line (Y^{79}) and *in silico* docking approaches

Elango Rajeswari[1], Balu Prakash[1]*, Durai Mahendran[2], Devarajan Natarajan[3]

[1]Department of Biotechnology, Vivekananda College of Arts and Science for Women (Autonomous), Namakkal, Tamil Nadu, India.
[2]Department of Biotechnology, Pavendar Bharathidasan College of Engineering and Technology, Tiruchirappalli, Tamil Nadu, India.
[3]Natural Drug Research Laboratory, Department of Biotechnology, Periyar University, Salem, 636011, Tamilnadu, India.

ARTICLE INFO

Article history:
Received on: May 01, 2024
Accepted on: August 01, 2024
Available online: September 16, 2024

Key words:
Tabernaemontana divaricate,
Apparicine,
Y^{79} human retinoblastoma cell line,
cytotoxicity,
in silico.

ABSTRACT

Tabernaemontana divaricata is a widely recognized traditional medicinal plant utilized for alleviating a variety of ailments. The objective of this study was to utilize nuclear magnetic resonance (NMR) techniques for the identification of bioactive compounds found in the flowers of *T. divaricata*. Furthermore, the study assessed the cytotoxic effects of the plant extracts on the Y^{79} cell line, which is a human retinoblastoma cell line in addition to focusing on the *in silico* molecular docking approach. The better result of column chromatography (CC) and thin layer chromatography (TLC) fraction was collected from chloroform: methanol in the ratio of 9.05:0.5 and 9:1. The isolated compound Apparicine was structurally confirmed by ^{1}H-NMR spectrum. ^{1}H-NMR spectrum of Apparicine revealed the presence of the olefinic group appearing at 5.45–5.75 ppm, and ^{13}C NMR spectrum of Apparicine revealed 17 carbon signals including 8 aromatics, 1 methyl, 4 methylene, and 4 olefinic carbons. Using mass spectrometry, the chemical Apparicine was confirmed when the molecular ions $[M^+H]^+$ peak were observed at 265.12 *m/z*. When the cytotoxic effect of Apparicine's bioactive constituent was examined using the 3-[4,5-dimethylthiazol-2-yl]-2,5 diphenyl tetrazolium bromide assay, it was shown that cell viability decreased as the concentration increased and the IC_{50} value of 26.88 µg/ml was reported. *In silico* molecular docking studies were conducted to analyze the Apparicine compound and determine its binding affinity with retinoblastoma proteins (1GUX, 2QDJ, 6KMJ, and 4YOO). The study demonstrated that Apparicine from *T. divaricata* possesses strong cytotoxicity and may be recommended as a ligand for cancer protein targets.

1. INTRODUCTION

Uncontrolled cell division and the spread of aberrant cells into surrounding tissues are hallmarks of the complicated disease known as cancer [1]. Retinoblastoma, which is the most common eye cancer in the world, primarily affects children under the age of 18 months, and 8000 new cases are reported each year. It is generated from the retinal tissue of the eyes [2-4]. Numerous alterations in both the environment and within organisms can lead to cancer. Most vertebrates, particularly mammals, have reduced amounts of CpG dinucleotide in their DNA. The remaining CpGs that group together in DNA areas are commonly called CpG islands (CGIs). The objective of this study was to assess gene expression analysis in cancer tissues because there has been an increasing interest in CGIs due to their enrichment in gene promoters, their ability to alter DNA methylation, and their crucial roles in controlling gene expression and silencing in biological processes such as X-chromosome inactivation, imprinting, and the silencing of intragenomic parasites. Additionally, CGIs may significantly aid in the discovery of epigenetic causes of cancer [5-8]. In 2020, as per the World Health Organization, cancer ranks as the second most common cause of death worldwide. Early detection and effective treatment must be accessible [9]. Treatments for retinoblastoma often involve radiation and chemotherapy, which can gradually harm good cells and increase their resistance to cancerous cells [3]. Current studies therefore concentrate on the possible therapeutic medication with the fewest possible adverse effects and several herbal medicines used in developed nations to address a wide range of health issues [3,10]. Plants produce a wide variety of phytochemicals and have rich sources of bioactive compounds such as alkaloids, phenolics, steroids, and terpenoids. Medicinal plants

*Corresponding Author:
Balu Prakash,
Department of Biotechnology,
Vivekananda College of Arts and Science for Women (Autonomous),
Namakkal, Tamil Nadu, India.
E-mail: prakazbt@gmail.com

are reported as potent anthelmintic, schizonticidal, anticancer, anti-inflammatory, antioxidant, ascaricidal, antibacterial, insecticidal, anti-diarrheal, and larvicidal activities [11-13]. *Tabernaemontana divaricata* (*Apocynaceae*) is native to India and its evergreen shrub is now grown all across Southeast Asia. The phytochemical contents of the plant have been reported from the stem, root, flower, and leaves containing flavonoids, phenylpropanoids, terpenoids, enzymes, and steroids. The pharmacological properties of the plant are reported as analgesic, anti-diarrhea, antioxidant, anti-inflammatory, and reversible acetylcholinesterase inhibition effects [14-16]. The creation of novel, least-toxic drug moieties involves computational methods. Computational modeling of drugs is predicated on an understanding of the ligand and target receptor [17]. The molecular structures of the ligands can be linked to the biological activity by the application of either structure-based or ligand-based molecular design techniques. Both of these strategies rely on ligand and receptor data that are readily accessible to the general public [18]. In medicinal chemistry, computational studies are regarded as important tools that can expedite the drug-design process [19]. As far as we are aware, no scientific data exist to support the claim that *T. divaricata* flower extract inhibits Y^{79} human retinoblastoma cells. Hence, this study aimed to isolate and structurally identify the bioactive compound from ethyl acetate flower extract of *T. divaricate* by chromatography elucidation method, thin layer chromatography (TLC), column chromatography (CC), spectral approach of Fourier infrared (FTIR) spectroscopy, proton nuclear magnetic resonance (^{1}H-NMR, ^{13}C-NMR), and liquid chromatography-mass spectrometry (LC-MS). The cell viability test of the purified compound was evaluated against Y^{79} human retinoblastoma cells by 3-[4,5-dimethylthiazol-2-yl]-2,5 diphenyl tetrazolium bromide (MTT) assay.

2. MATERIALS AND METHODS

2.1. Plant Collection and Identification

Fresh and healthy *T. divaricata* flowers were collected from fields in the Salem District (latitude 11.2189°N, longitude 78.1674°E), India. Botanical Survey of India recognized and verified the plant (Southern Circle), Govt. of India (BSI/SRC/Tech/317), and there is a voucher specimen in the herbarium of Vivekananda Women's College, Tiruchengode.

2.2. Preparation of Plant Extraction

Ten days of 12/12 light/dark cycles were used to air-dry the harvested plant blooms at 25°C. After 10 days, the plant material was powdered using a mechanical blender, sieved with a 40-m screen, and kept in an airtight container. Using 250 mL of each polar solvent, 48 h was spent sequentially extracting 50 g of powder, such as chloroform, ethyl acetate, and acetone as well as hexane and chloroform based on the polarity. The independently obtained extracts were concentrated at 40°C under low pressure using a rotary evaporator until further analysis, and the extract yield of the molecules was measured [20].

2.3. Qualitative Analysis of Phytochemical Screening

The preliminary phytochemical analysis of *T. divaricata* flower extracts of various solvents, alkaloids, flavonoids, phenols, tannins, saponins protein, steroids, carbohydrates, and glycosides were screened by the standard procedure described earlier [21-24].

2.4. Thin Layer Chromatography

The TLC profile for ethyl acetate floral extract of *T. divaricata* was eluted in a closed tank with a lidded system. The process was repeated with more strips, and other polar and non-polar ratios were employed to raise the more polar solvent content by 10% until the plates with the different solvent–solvent ratios to the proper resolution such as hexane: ethyl acetate (7:3, 6:4, 5:5) chloroform: methanol (9.05:0.5, 9:1) and ethyl acetate: methanol (9:1) were used in this study. Through capillary action, the solvent moved up the plate at the top. Before the strip was examined by spraying silver nitrate and seeing the iodine vapor under a UV lamp, the cover was removed and the strip was dried. The *Rf* (retention factor) values of the purified compounds were calculated [25,26].

2.5. Column Chromatography

The crude extracts of *T. divaricata* flower were eluted through CC to identify the pure compound. Chloroform: methanol ratio of 100%, 80%, 70%, 60%, and 50% can be achieved by increasing the amount of polar solvent in the solvent by the 20% system. The collected fractions of CC were further purified by preparative TLC over a 0.25-mm layer of silica gel GF-254. The active compound was separated into chromatographic solvents using chloroform: methanol at room temperature [27].

2.6. FTIR Analysis

To identify the many types of chemical linkages (functional groups) found in compounds, FTIR is a potentially useful technique. Additionally, a molecule's structure can be determined using the functional groups present in the flower extract of *T. divaricata.* At room temperature, floral extracts were subjected to FTIR measurement using a Perkin Elmer spectrophotometer. After milling and combining the spectroscopic grade KBr solution with around 3 mg of compound chemical, the pellet was formed. From 4000 to 400 cm^{-1}, the FTIR spectrum was captured [28]. The FTIR analysis of the sample was done in the Central Instrumental Facility, St. Joseph's College (Autonomous), Tiruchirappalli, Tamil Nadu, India.

2.7. NMR of Compound

Protons and carbon atoms of the isolated compound were determined using the NMR spectrum. Atoms and fragments of compounds were identified using ^{1}H-NMR and ^{13}C-NMR in ^{1}D-NMR analysis. In NMR investigations, tetramethylsilane served as the internal standard, and samples weighing 10–30 mg were dissolved in a deuterated solvent. For the determination of the signals, ppm and chemical shifts were used; ppm for ^{1}H-NMR and ^{13}C-NMR and spectrum widths of 0–12 and 0–220 ppm are typical values. This study was carried out at SASTRA University in Tanjore, Tamil Nadu, India. After comparing the graph results with the reference chart, it was feasible to identify any potential functional groups that the plant may have [29].

2.8. LC-MS Techniques of Compound

Recording mass spectrometry required the dissolution of 0.04 mg (0.4 mg) of crude chemical in 10 mL methanol: acetonitrile (7:3). ESI was used in a C^{18} column with a flow rate of 0.5 mL/min for 45 min to record mass spectra of crude and isolated compounds using the Waters-Synapt G2 instrument [30].

2.9. Cell Line and Culture Condition

The human Y^{79} retinoblastoma cells from India's National Center for Cell Science were used in the experiment (NCCS). For 24 h, the acquired stock cells were cultured in Dulbecco's Modified Eagle

Media (DMEM) supplemented with streptomycin penicillin, and 10% fetal bovine serum (FBS) was added to 95% air in a humidified environment with 5% CO_2 until the cells reached mingling at 37°C.

2.10. Cell Seeding

Seeding of cells and cell detaching solution (trypsin 0.02%, ethylenediaminetetraacetic acid 0.02%) and glucose (0.05%) in PBS were used to separate the cells. After the cell viability was determined, they were centrifuged, seeded at a density of 50,000 cells per well in a 96-well plate, allowed to grow in a monolayer under usual conditions, and then harvested for cytotoxicity studies.

2.11. Cell Viability Assay of the Compound

The cancer cell viability test of the isolated chemical was assessed using the MTT assay [31,32]. Briefly, Y^{79} cells (5×10^3 cells/ml) were plated in 96-well plates with DMEM medium containing 10% of FBS. The cells were incubated for 24 h under 5% CO_2, 95% O_2, and 100% relative humidity at 37°C. After the medium was taken out, serum-free medium was added, and PBS was used to wash it. Serum-free media was given to the control cells, while the treatment cells were given medium containing 50, 100, 150, 200, and 250 µg/mL of the pure substance Apparicine. The culture plates were then incubated for an additional 3 h, after which the supernatant was decanted. About 100 µl dimethyl sulfoxide (DMSO) was added, and the created crystal was carefully dissolved using two to three pipetting. The absorbance was measured using a microplate reader (SPECTRA AX I3) at a wavelength of 570 nm. The dose–response curves yielded the IC_{50} values, from which the percentage growth inhibition was computed:

$$\text{Growth inhibition}\,(\%) = \frac{A_{570}\,\text{of treated cells}}{A_{570}\,\text{of control cells}} \times 100$$

2.12. Cell Morphological Study

Through the use of a human retinoblastoma (Y^{79}) cell line, the isolated Apparicine compound of *T. divaricata* underwent morphological alterations that were observed under a microscope. The Y^{79} cells line (5×10^4 cells/ml) were plated in 96 well plates with Dulbecco's modified eagle medium (DMEM) containing 10% FBS. After the medium was taken out, fresh medium was added to the control plates, and 50, 150, and 250 µg/mL of Apparicine compound were added to the treatment dishes. After the culture plates were cultured for 2 days, the cells were seen and captured on camera using an inverted light microscope, with a magnification of 20×.

2.13. *In Silico* Molecular Docking Study

In silico molecular docking studies were conducted to investigate the interaction between the Apparicine compound and retinoblastoma protein (1GUX, 2QDJ, 6KMJ, and 4YOO) molecules using Autodock.

2.13.1. Ligand preparation

Apparicine ligand molecules were selected to study their interactions with the four retinoblastoma protein molecules (1GUX, 2QDJ, 6KMJ, and 4YOO). The three-dimensional (3D) structure of Apparicine was retrieved from the Pub Chem database, with PubChemID5281349 [33]. Using Open Babel 2.3.2, ligand structures were translated from the sdf format to the pdb format [34]. The most stable conformations of the ligand structures were achieved by minimizing their energy using Merck Molecular Force Field – MMFF94 [35]. The Avogadro software was used to minimize energy [36]. The structure was saved in the "pdb" format so that MGLTools-1.5.6 could convert the ligand structure into the proper input file format (pdbqt) for docking studies [37-39].

2.14. Statistical Analysis

One-way analysis of variance and the least significant difference test were used to statistically assess the study's data, and p-values of less than 0.01 were considered statistically significant. The MTT assay data were presented as the mean ± SD of experiments conducted SEM of three replicates, and the IC_{50} (50% inhibition of cell proliferation) values were calculated using the Graph Pad Prism software.

3. RESULTS

3.1. Preliminary Phytochemical Screening

The screening of phytochemicals extract was determined through qualitative identification of various secondary metabolites present in *T. divaricata*, and the results showed the presence of saponins, phenols, tannins, flavonoids, and alkaloids in all solvent extracts [Table 1]. The results of extraction yield from every fraction of *T. divaricata* were summarized [Table 2]. The highest yield was achieved from the ethyl acetate extract (21.50%) followed by methanol (15.74%) and hexane (7.12%).

3.2. TLC and CC

The sample was applied to chromatographic separation for eluted various fractions of crude ethyl acetate extract. Based on the TLC profile, the solvent system was chosen for CC (silica gel $60G_{254}$). The fraction bands will move down the column along with the (9.05:0.5, 9:1), and $CHCl_3$: MeOH was chosen as the CC solvent system [Figure 1]. CC was performed on a pack of silica gel (60–120 mesh) with 20 g of the extract. The methodical order in which the solvents are chosen demonstrates how polarity affects extraction. Totally,

Table 1: Preliminary phytochemical screening of the various solvent extracts of *T. divaricata* flower.

S. No.	Phytochemicals	Hexane	Ethyl Acetate	Methanol
1.	Alkaloids	+	+	+
2.	Flavonoids	+	+	+
3.	Phenolics	+	+	+
4.	Proteins	–	–	–
5.	Steroids	–	–	–
6.	Tannins	+	+	+
7.	Saponins	+	+	+
8.	Carbohydrate	+	+	–
9.	Glycosides	–	–	+

"+" Present; "–" absent.

Table 2: Weight and extractive yield of the crude of *T. divaricata*.

Solvent	Weight of Crude Extract (g)	Yield (%)
Hexane extract	7.12	14.24
Ethyl acetate extract	10.75	21.50
Methanol extract	7.87	15.74

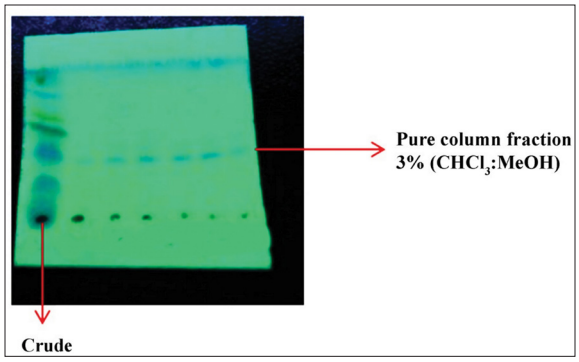

Figure 1: Column purification of ethyl acetate crude.

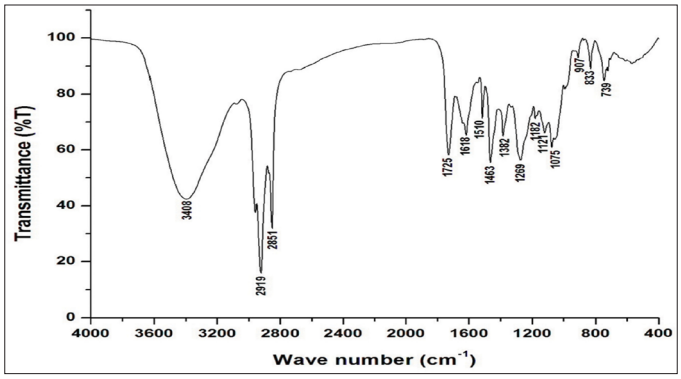

Figure 2: FT-IR spectrum of ethyl acetate flower extract of *T. divaricata*.

Table 3: Functional groups in ethyl acetate flower extract of *T. divaricata* by FTIR analysis.

Frequency (cm^{-1})	Frequency Range	Bond	Functional Group
3408	3550–3150	N–H stretching	Indole
2919	2900–3000	C–H stretching	Methyl and methylene
2851	2850–2800	C–H stretching	Methyl and methylene
1618	1630–1600	C=C stretching	Olefinic group
1463	1550–1400	C=C stretching	Olefinic group
1121	1150–950	C–N stretching	Tertiary amine
1510	1550–1500	C–C stretching	Aromatic group
1075	1100–900	C–H bending	Plane of aromatic
739	700–500	C–H bending	Aromatic

Table 4: NMR data of isolated compound, Apparicine.

S. No.	^{1}H-NMR ppm	^{13}C-NMR ppm
1.	1.51(2H)	13.5
2.	2.01(3H)	34.1
3.	2.18(2H)	44.9
4.	3.11(1H)	51.9
5.	4.02(2H)	53.5
6.	4.34(1H)	111.3
7.	4.67(1H)	115.8
8.	4.90(1H)	116.0
9.	5.45–5.75(2H)	118.4
10.	7.00(1H)	119.5
11.	7.13(1H)	123.1
12.	7.34(2H)	123.6
13.	11.16(1H)	128.4
14.	–	133.0
15.	–	134.5
16.	–	136.1
17.	–	141.6.

75 fractions were concentrated, and the fractions were collected in individual containers. Among 75 fractions, 3 were selected for the purity check using other spectral studies used to determine whether a single compound was present. The Spot of each fraction was noted on a TLC plate. TLC plates were fabricated by using chloroform and methanol (9.5:0.5) mixtures. Three fractions were visualized by the high (254 nm) range of the UV spectrum. The *Rf* value of separated fractions 1, 2, and 3 was calculated at 0.1, 0.25, and 0.5 cm, respectively.

3.3. FTIR Spectroscopy

The FTIR spectrum results proved the existence of functional groups in the ethyl acetate extract flower of *T. divaricata* [Table 3]. The isolated compound exhibits a characteristic band at 3408 cm^{-1} indicating the presence of indole N–H stretching. The absorption of major peaks was observed at the band of C–H of Apparicine at 2919 cm^{-1}; 2851 cm^{-1} in the spectrum indicated the methyl and methylene groups in the chemical structure. Double-bond C=C stretching frequency observed at 1618 and 1463 cm^{-1} may represent the olefinic group in the suggested structure. The tertiary amine C–N stretch was observed at 1121 cm^{-1}, and an aromatic C–C stretch was observed at 1510 cm^{-1}. The peaks observed at 1075 cm^{-1} and 739 cm^{-1}, there was a difference due to the stretching in the plane and the bending out of the plane of aromatic C–H [Figure 2].

3.4. NMR Spectroscopy

The isolated compound Apparicine structurally confirms that the ^{1}H-NMR and ^{13}C-NMR were used [Table 4]. The resulting chemical shift value of Apparicine is as follows: ^{1}H-NMR, DMSO-d_6: 1.51(2H), 2.01(3H), 2.18(2H), 3.11(1H), 4.02(2H), 4.34(1H), 4.67(1H), 4.90(1H), 5.45-5.75(2H), 7.00(1H), 7.13(1H), 7.34(2H), and 11.16(1H). ^{1}H-NMR spectrogram of Apparicine revealed the presence of the olefinic group appearing at δ 5.45–5.75 ppm. One methyl group present in the Apparicine is resonated at δ 2.01 ppm. All the aromatic protons of Apparicine were observed between 7.00 and 7.34 parts per million (ppm). The indole N–H was observed as a broad peak at δ 11.16 ppm [Figure 3].

The ^{13}C-NMR spectrum chemical shift values are as follows: ^{13}C NMR, DMSO-d_6: 13.5, 34.1, 44.9, 51.9, 53.5, 111.3, 115.8, 116.0, 118.4, 119.5, 123.1, 123.6, 128.4, 133.0, 134.5, 136.1, and 141.6. The ^{13}C-NMR spectrum of Apparicine showed methyl group carbon at δ 13.5 ppm. The olefinic carbon was observed at δ 118.4, 119.5, 133.0, and 141.6 ppm. The ^{13}C NMR spectrum of Apparicine revealed 17 carbon signals including 8 aromatics, 1 methyl, 4 methylene, and 4 olefinic carbons [Figure 4]. The determination of biological activities of the olefinic group at 5.45–5.75 ppm Apparicine ^{1}H-NMR spectrogram demonstrated the functional group of presence, and methyl group

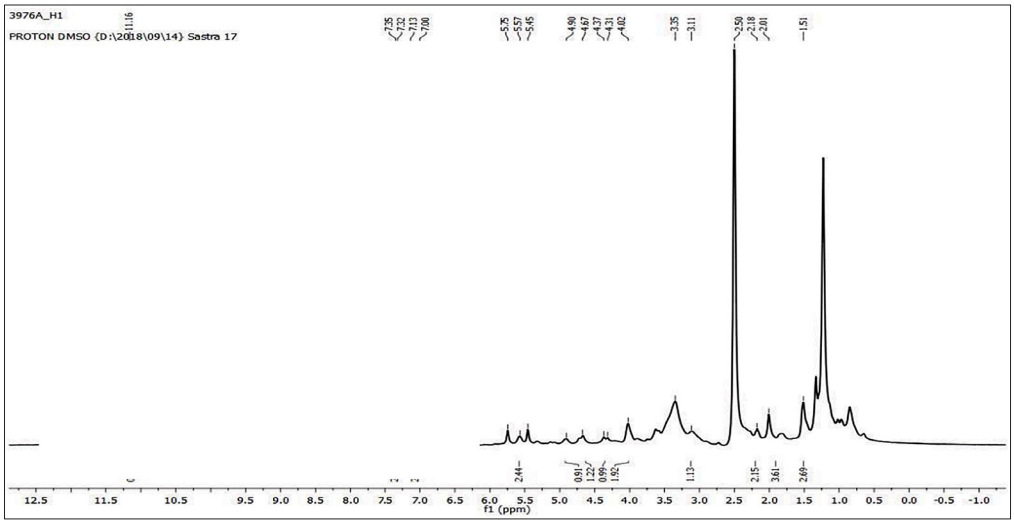

Figure 3: [1]H-NMR spectrum of Apparicine.

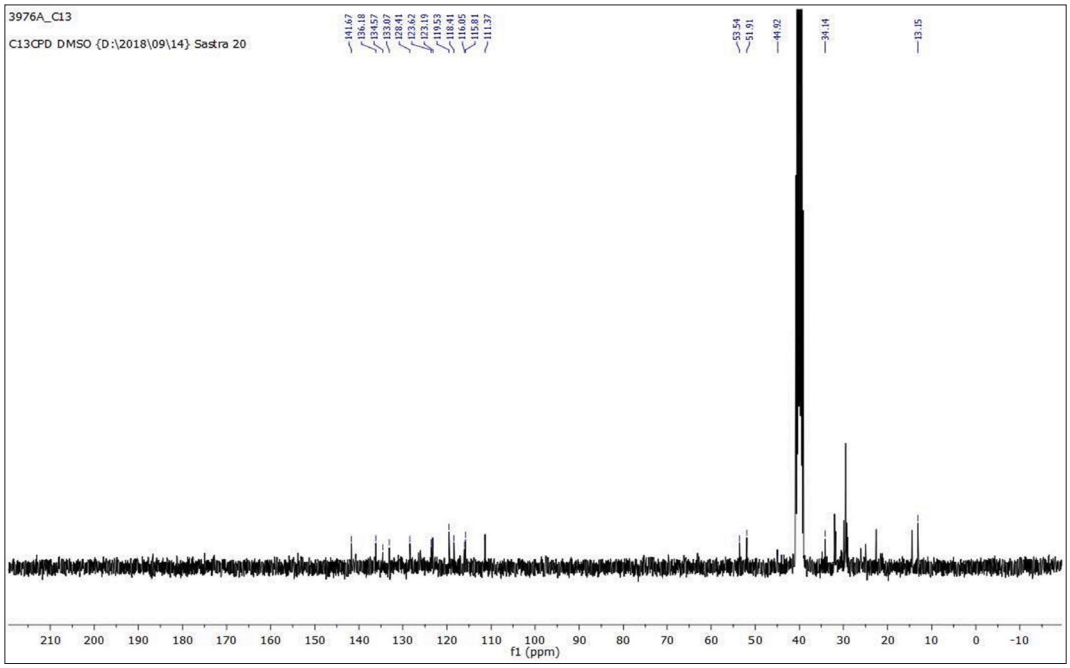

Figure 4: [13]C NMR spectrum of Apparicine.

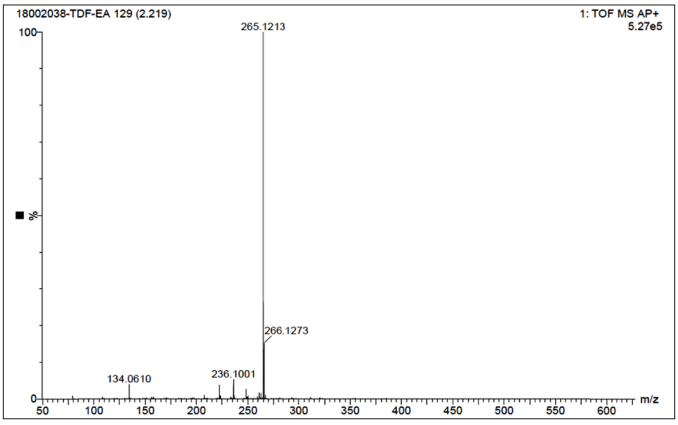

Figure 5: Mass spectrum of Apparicine.

carbon was visible in the Apparicine [13]C-NMR spectra at a level of about 13.5 ppm.

3.5. Mass Spectroscopy

Mass spectroscopy results showed that the ion in a molecule $[M^{+}H]^{+}$ peak was obtained at 265.12 *m/z*, which confirms the compound Apparicine. It was proposed that the structure may be Apparicine. The mass spectrum of Apparicine is shown in Figure 5, and the compounds were identified by LC-MS, [1]H-NMR, [13]C-NMR, and FTIR.

3.6. Cytotoxic Activity

The cytotoxic effects of different concentrations of isolated Apparicine compound (50, 100, 150, 200, and 250 µg/ml) from the flower extract of *T. divaricata* were investigated using a normal

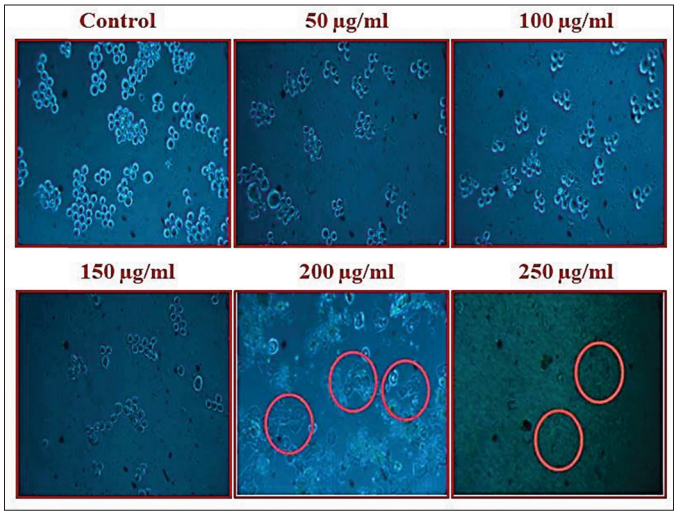

Figure 6: Morphological effect for bioactive Apparicine compound isolated from ethyl acetate flower extract of *T. divaricata* on Y^{79} cell line.

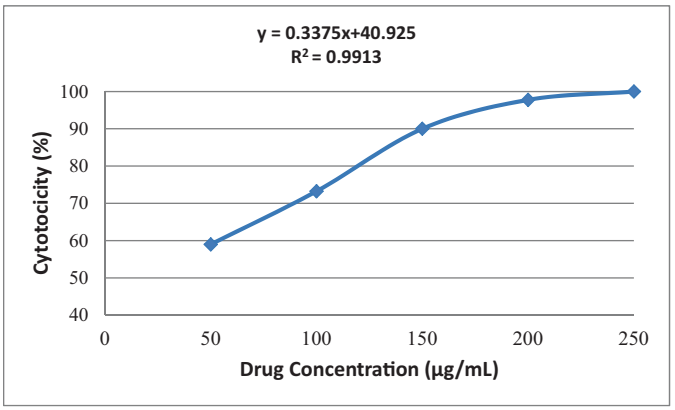

Figure 7: Cell viability percentage for bioactive Apparicine compound from ethyl acetate flower extract of *T. divaricata* on Y^{79} cell line. The results show a statistically significant difference ($p < 0.01$) between control cells treated with the Apparicine compound.

Table 5: Cytotoxicity of the Apparicine against retinoblastoma cell line.

Concentration (µg/ml)	Cytotoxicity (%)	Viability (%)	Reactivity
50	65	35	Moderate
100	65	35	Moderate
150	70	30	Moderate
200	76	24	Severe
250	90	10	Severe

human retinoblastoma (Y^{79}) cell line. The results expressed that the morphological changes and damages in the cells treated occurred in a dose-dependent manner, meaning that the viability of cells decreased steadily as the chemical concentration increased [Figure 6]. The percentages of cell viability for different concentrations of test samples (50, 100, 150, 200, and 250 µg/mL) are shown in Figure 7. The viability of cells declined more rapidly than at 50 µg/ml. A concentration of up to 50–250 µg/mL yielded an IC_{50} value of 26.88, and the percentage cell viability for the purified Apparicine bioactive component isolated from *T. divaricata* flower extract was reported to be 0.991 R^2 value. The results for Apparicine on cell lines were statistically significant at $p < 0.01$* when comparing control cells with cells treated with Apparicine molecule. The cytotoxicity activity of pure compound shows a decreasing viability of cancer cells by increasing the Apparicine concentration by 50–250 µg/mL [Table 5].

Table 6: Interacting residues between receptor molecules and lead compound.

Name of the Compound	PDB ID	Target Protein	Binding Site	Bond Length	Binding Energies (kcal/mol)
Apparicine	1GUX	Retinoblastoma protein	TRP A:516	4.89	–7.3
				5.34	
			MET A:495	4.11	
				4.17	
			ARG A:445	4.97	
				4.26	
	2QDJ	Retinoblastoma-associated protein	LYS A:329	4.58	–8
			VAL A:108	5.26	
			PHE A:104	5.01	
	6KM7	Retinoblastoma-binding protein 5	ARG A:34	4.93	–8.2
				5.01	
			ARG A:161	5.43	
			ARG A:208	5.09	
			PRO A:117	5.06	
			LEU A:491	4.57	
	4YOO	Retinoblastoma-like protein 1	PHE A:497	3.53	–8.1
				4.89	
			LYS A:535	5.04	
				4.39	
			ILE A:496	5.25	
				4.40	
			VAL A:536	5.35	

3.7. Molecular Docking Studies

3.7.1. Ligand–receptor interaction

The results of the docking analysis provided a reasonable explanation for the differences in inhibitor activity observed among the compounds, suggesting that the actual binding mode of tiny molecules may be represented by the predicted binding mode. Thus, molecular docking could serve as an essential tool for preliminary predicting inhibitor activity for the future design of small molecules. Specifically, when choosing newly created small molecules' docking findings, the information obtained from this study could be used as a reference. One compound was tested for its binding energy with four proteins (1GUX, 2QDJ, 6KMJ, and 4YOO) to demonstrate the application of molecular docking. The results showed that Apparicine binding energy with 1GUX –7.3, 2QDJ –8.0, 6KMJ –8.2, and 4YOO –8.1 kcal/mol was also identified as electronegative regions and hydrogen-bond receptor residues [Table 6; Figure 8].

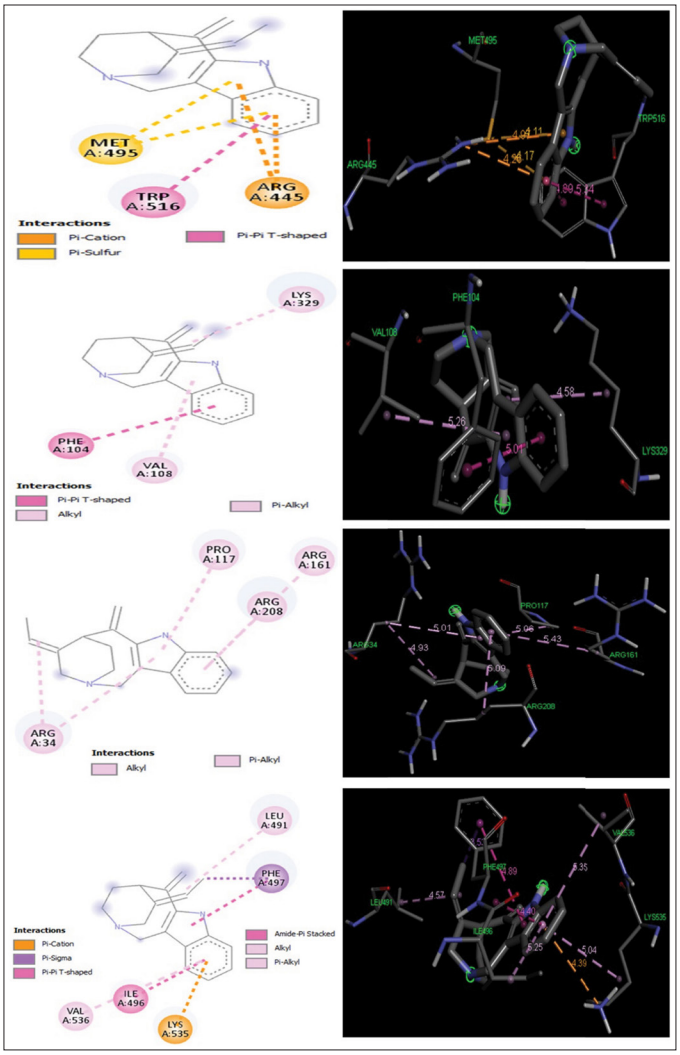

Figure 8: 2D and 3D interaction of amino acid diagram of the Apparicine selected compounds in the identified active site.

4. DISCUSSION

The phytochemical constituents are recognized for their diverse biological activities, encompassing anti-inflammatory, anti-tumor, and antioxidant properties [40,41]. The flower of *T. divaricata* was subjected to extraction yield calculations using hexane, ethyl acetate, and methanol extracts. According to the findings, the ethyl acetate extract produced the most percentage. The weight of crude extract and yield of the crude of other plants have been reported by researchers [42,43], and this study noted that the highest yield of Apparicine from the ethyl acetate extract suggests its abundance in *T. divaricata* and underscores its potential medicinal significance. A good solvent solution is necessary for the effective separation of biomolecules using chromatographic techniques, and each target compound's optimal range of partition coefficient must be met [44]. The chromatographic techniques, including TLC and CC, played a crucial role in isolating the bioactive compound, Apparicine, from the *T. divaricata* extract. TLC revealed the presence of phenolic compounds, which are often associated with beneficial health effects and may contribute to the observed cytotoxic activity [45,46]. TLC chromatograms of plant extract revealed the presence of phenolic chemicals. Using its *Rf* value, one fraction successfully demonstrated the presence of bioactive chemicals. Additionally, two compounds (such as D4 and D5) that were obtained through the chromatographic separation and distillation of the methanolic extracts from *Schefflera stellata* leaves exposed the presence of bioactive chemicals, with *Rf* values of D4 –0.44, 0.54, 0.71, and D5 0.76 [32]. The results of this investigation showed that the primary functional group of methyl and methylene group present in *T. divaricata* is the C–H bond. FTIR spectroscopy verified that Apparicine contains distinctive functional groups, including indole N–H stretching, C–H stretching (methyl and methylene groups), and C=C stretching (olefinic group). Similar kinds of functional groups were reported from the different plant species. These spectral signatures were related to the structure of Apparicine [47,48]. According to previous research, the indole group and its derivatives were evaluated for cytotoxic activity utilizing cancer and normal cell lines in the MTT assay with conventional medication [49]. The NMR spectra provided further evidence supporting the identification of Apparicine. The presence of an olefinic group, methyl groups, and aromatic protons in the ^{1}H-NMR spectra, along with specific carbon signals in the 13C NMR spectra, substantiated the structure of Apparicine [50,51]. Mass spectrometry results further validated the identity of Apparicine with the detection of the molecular ion peak at 265.12 *m/z*. The findings of this study were correlated with previous reports on Apparicine's mass spectrum [52,53]. The Apparicine compound isolated from the plant is comparable with the findings of this investigation. *T. divaricata* was reported by other researchers [54] who isolated Apparicine from the stem of a medicinal plant [55] and reported that the *T. divaricata* leaves contain alkaloids glycorine, glycosmicine, glycophymine, glycophymoline, and glycomide. Similarly, the same compound was isolated from *Glycosmisarborea* [56], and the compound showed promising anticancer activity against various cancers. According to the current investigation, the Apparicine compound is cytotoxic to the human retinoblastoma (Y^{79}) cell line**.** The cytotoxic activity of Apparicine against human retinoblastoma (Y^{79}) cells was assessed, and the compound showed a dose-dependent decrease in the viability of the cells. The findings of this study are consistent with earlier research, indicating that Apparicine and its derivatives may have anticancer properties [57,58]. Virtual screening techniques are commonly and extensively used to reduce the expense and duration of medication development. Molecular docking is a key tool in structure-based drug design, as it discovers novel ligands for protein structures [59]. When formulating medications, the interaction between the chemicals and the receptor is crucial. Many human disorders, such as cancer and inflammatory conditions, can be treated with natural compounds, and many medications are made from them. Similarly, research has demonstrated that hydrogen bonds and hydrophobic interactions both considerably increase the stability of a compound. Thus, the results of this study demonstrate the usefulness of molecular docking analysis in understanding the mechanisms of binding between small molecules and proteins. The findings obtained from this research can serve as a useful guide for designing new small molecules with enhanced inhibitor activity [60].

5. CONCLUSION

This research concluded that the phytochemical study indicates that *T. divaricate* flowers are a potential source of beneficial compounds. This is the first report on the cytotoxic effects of Apparicine compound on human retinoblastoma cells, specifically on Y^{79} cells. This study concludes that *T. divaricata* contains a variety of bioactive chemicals. Among these, the bioactive compound Apparicine was successfully isolated and described as a substantial component with promising

cytotoxic action against human retinoblastoma cells. The results establish a foundation for additional investigation into the potential therapeutic applications of *T. divaricata* and its bioactive constituents within the oncology domain.

6. ACKNOWLEDGMENTS

The authors thank Vivekananda College of Arts and Science for Women (Autonomous), Namakkal, Tamil Nadu, India, for providing a laboratory facility for the successful completion of this research work.

7. AUTHOR CONTRIBUTIONS

The corresponding author can provide all data or analyses used in this study that were published in the article upon reasonable request. BP conceptualized this study, whereas ER designed the experiments. Data interpretation was carried out by BP, DM, and ER. Each author prepared, read, and approved the final work to some extent.

8. FINANCIAL SUPPORT AND SPONSORSHIP

There is no funding to report.

9. CONFLICTS OF INTEREST

The authors report no financial or any other conflicts of interest in this work.

10. ETHICS APPROVAL

This study does not involve experiments on animals or human subjects.

11. DATA AVAILABILITY

All the data is available with the authors and shall be provided upon request.

12. USE OF ARTIFICIAL INTELLIGENCE (AI)-ASSISTED TECHNOLOGY

The authors confirm that there was no use of artificial intelligence (AI)-assisted technology for assisting in the writing or editing of the manuscript and no images were manipulated using AI.

13. PUBLISHER'S NOTE

All claims expressed in this article are solely those of the authors and do not necessarily represent those of the publisher, the editors and the reviewers. This journal remains neutral with regard to jurisdictional claims in published institutional affiliation.

REFERENCES

1. De Greef D, Barton EM, Sandberg EN, Croley CR, Pumarol J, Wong TL, et al. Anticancer potential of garlic and its bioactive constituents: a systematic and comprehensive review. In: Seminars in cancer biology. Academic Press; 2021. p. 219–64. (vol 73).
2. Kivela T. The epidemiological challenge of the most frequent eye cancer: retinoblastoma, an issue of birth and death. Br J Ophthalmol. 2009;93:1129–31.
3. Kamarudin AA, Sayuti NH, Saad N, AbRazak NA, Esa NM. Induction of apoptosis by *Eleutherinebulbosa* (Mill.) Urb: bulb extracted under optimised extraction condition on human retinoblastoma cancer cells (WERI-Rb-1). J Ethnopharmacol. 2022;284:114–770.
4. Fernandes AG, Pollock BD, Rabito FA. Retinoblastoma in the United States: a 40-year incidence and survival analysis. J Pediatric Ophthalmol Strabismus. 2018;55(3):182–8.
5. Barazandeh A, Mohammadabadi MR, Ghaderi-Zefrehei M, Nezamabadipour H. Genome-wide analysis of CpG islands in some livestock genomes and their relationship with genomic features. Czech J Anim Sci. 2016;61:487.
6. Barazandeh A, Mohammadabadi MR, Ghaderi-Zefrehei M, Nezamabadipour H. Predicting CpG Islands and their relationship with genomic feature in cattle by hidden Markov model algorithm. Iran J Appl Anim Sci. 2016;6(3):571–9.
7. Mohammadabadi MR, Mozafari MR. Enhanced efficacy and bioavailability of thymoquinone using nanoliposomal dosage form. J Drug Deliv Sci Technol. 2018;47(1):445–53.
8. Zarrabi A, Alipoor Amro Abadi M, Khorasani S, Mohammadabadi MR, Jamshidi A, Torkaman S, et al. Nanoliposomes and tocosomes as multifunctional nanocarriers for the encapsulation of nutraceutical and dietary molecules. Molecules. 2020;25(3):638.
9. Imane B, Laila B, Fouzia H, Ismail G, Ahmed E, Kaoutar B, et al. Chemical characterization: antiproliferative activity and molecular docking of bioactive compounds from brown algae Fucusspiralis. Algal Res. 2022;68:102887.
10. Yadav M, Bhatia VJ, Doshi G, Shastri K. Novel techniques in herbal drug delivery systems. Int J Pharmaceut Sci Rev Res. 2014;28:83–9.
11. Mani JS, Johnson JB, Hosking H, Ashwath N, Walsh KB, Neilsen PM, et al. Antioxidative and therapeutic potential of selected Australian plants: a review. J Ethnopharmacol. 2021;268:113580.
12. Patra JK, Thatoi HN. Metabolic diversity and bioactivity screening of mangrove plants: a review. Acta Physiol Plant 2011;33:1051–61.
13. Alabi, MA, Muthusamy A, Kabekkodu SP, Adebawo OO, Satyamoorthy K. Anticancer properties of recipes derived from Nigeria and African medicinal plants on breast cancer cells *in vitro*. Scient Afr. 2020;8:e00446.
14. Pushpa B, Latha KP, Vaidya VP, Shruthi A, Shweatha A. Phytochemical analysis and antimicrobial evaluation of leaves extract of *Tabernaemontana coronaria*. J Chem Pharm Res. 2012;4:3731–3.
15. Gopinath SM, Suneetha TB, Mruganka VD, Ananda S. Evaluation of antibacterial activity of *Tabernaemontana divaricata (L.)* leaves against the causative organisms of bovine mastitis. Int J Res Phytochem Pharmacol. 2011;1(4):211–3.
16. Poornima K, Krishnan R, Aswathi KV, Gopalakrishnan VK. Toxicological evaluation of ethanolic extract of *Tabernaemontana coronaria (L) R. Br*. Asian Pac J Trop Dis. 2012;2:S679–84.
17. Correa-Basurto J, Bello M, Rosales-Hernandez MC, Hernández-Rodríguez M, Nicolás-Vázquez I, Rojo-Domínguez A, et al. QSAR, docking, dynamic simulation and quantum mechanics studies to explore the recognition properties of cholinesterase binding sites. Chem Biol Interact. 2014;209:1–13.
18. Wang Z, Cheng L, Kai Z, Wu F, Liu Z, Cai M. Molecular modeling studies of atorvastatin analogues as HMGR inhibitors using 3D-QSAR, molecular docking and molecular dynamics simulations. Bioorg Med Chem Lett. 2014;24:3869–76.
19. Singh A, Goyal S, Jamal S, Subramani B, Das M, Admane N, et al. Computational identification of novel piperidine derivatives as potential HDM2 inhibitors designed by fragment-based QSAR,

molecular docking and molecular dynamics simulations. Struct Chem. 2016;27:993–1003.
20. Chethankumara GP, Nagaraj K, Krishna V, Krishnaswamy G. Isolation, characterization and *in vitro* cytotoxicity studies of bioactive compounds from *Alseodaphne semecarpifolia Nees*. Heliyon. 2021;7(6).
21. Kamal T, Muzammil A, Akintunde R, Rahma MS, Omar MN. Preliminary phytochemical screening test of *Garcinia griffithii* plant. Innova Ciencia. 2012;4(4):68–74.
22. Alfalluos KA, Alnade HS, Kollab WA, Alafid F, Edrah SM. Qualitative and quantitative phytochemical analysis and antimicrobial activity of "retama" extract grown in Zliten Libya. Int J Med Sci Clin Invent. 2017;4(4):2861–6.
23. Thilagavathi T, Arvindganth R, Vidhya D, Dhivya R. Preliminary phytochemical screening of different solvent mediated medicinal plant extracts evaluated. Int Res J Pharm. 2015;6(4):246–8.
24. Yunitasari N, Swasono RT, Pranowo HD, Raharjo TJ. Phytochemical screening and metabolomic approach based on Fourier transform infrared (FTIR): identification of α-amylase inhibitor metabolites in *Vernonia amygdalina* leaves. J Saudi Chemical Soc. 2022;26(6):101540.
25. Sadasivam S, Manickum A. Biochemical methods. New Age Intern (P) Ltd. Publication; 2005. p. 284–8.
26. Kumar T, Ray S, Brahmachary RL, Ghose M. Preliminary GC-MS analysis of compounds present in the root exudates of three mangrove species. Acta Chromatographica. 2009;21(1):117–25.
27. Pandey D, Gupta AK. Bioactive compound in *Curcuma caesia (Roxb.)* from Bastar and its spectral analysis by HPLC UV-visible FT-IR NMR and ESI-MS. Int J Pharma Sci Res. 2019;10:139–47.
28. Piruthiviraj P, Margret A, Krishnamurthy PP. Gold nanoparticles synthesized *by Brassica oleracea (Broccoli)* acting as antimicrobial agents against human pathogenic bacteria and fungi. Appl Nanosci. 2016;6:467–73.
29. Khan MSA, Ahmed N, Arifuddin M, Zakaria ZA, Al-Sanea MM, Khundmiri SUK, et al. Anti-nociceptive mechanisms of flavonoids-rich methanolic extract from *Terminalia coriacea (Roxb.)* Wight &Arn, leaves. Food Chemical Toxicol. 2018;115:523–31.
30. De Feo M, Paladini A, Ferri C, Carducci A, Del Pinto R, Varrassi G, et al. Anti-inflammatory and anti-nociceptive effects of cocoa: a review on future perspectives in treatment of pain. Pain Ther. 2020;9:231–40.
31. Mosmann T. Rapid colorimetric assay for cellular growth and survival: application to proliferation and cytotoxicity assays. J Immunol Methods. 1983;65(1-2):55–63.
32. Ramakrishnan R, Thangaswamy S, Balasubramaian MG, Rajamanickam M, Srinivasan N, Ganesan DS. Bioactive Compounds of *Schefflera stellata (Geartn) Baill.* leaf methanolic extract and their cytotoxic effect on lung cancer cell line (A549). Indian J Pharmaceut Educ Res. 2022;56(3):S469–78.
33. Kim S, Chen J, Cheng T, Gindulyte A, He J, He S, et al. PubChem 2019 update: improved access to chemical data. Nucleic Acids Res. 2019;47(D1):D1102–9.
34. O'Boyle NM, Banck M, James CA, Morley C, Vandermeersch T, Hutchison GR. Open babel: an open chemical toolbox. J Cheminformatics. 2011;3(1):33.
35. Hanwell MD, Curtis DE, Lonie DC, Vandermeersch T, Zurek E, Hutchison GR. Avogadro: an advanced semantic chemical editor, visualization, and analysis platform. J. Cheminformatics. 2012;4(1):17.
36. Halgren TA Merck molecular force field. I. Basis, form, scope, parameterization, and performance of MMFF94. J Comput Chem. 1996;17(5 6):490–519.
37. Sanner MF, Olson AJ, Spehner JC. Reduced surface: an efficient way to compute molecular surfaces. Biopolymers. 1996;38(3):305–20.
38. Sanner MF. Python: a programming language for software integration and development. J Mol Graph Model. 1999;17:57–61.
39. Morris GM, Huey R, Lindstrom W, Sanner MF, Belew RK, Goodsell DS, et al. AutoDock4 and AutoDockTools4: automated docking with selective receptor flexibility. J Comput Chem. 2009;30:2785–91.
40. Li X, Jiang H, Qu L, Yao J, Ma L, Wang X, et al. Phenolic compounds from *Tabernaemontana divaricata* and their anti-inflammatory activities. J Nat Prod. 2019;82(6):1671–81.
41. Ahmed M, Hossain MS, Mahal MJ, Islam MA, Hasan CM. Phytochemical investigation and bioactivities of *Tabernaemontana divaricata* (Linn.) leaves. J Pharm Negative Results. 2011;2(1):6–11.
42. Paulsamy S, Jeeshna MV. Preliminary phytochemistry and antimicrobial studies of an endangered medicinal herb *Exacum bicolor Roxb*. Res J Pharmaceut Biolog Chemic Sci. 2011;2(4):447–57.
43. Thaniarasu R, Anitha A. Phytochemical screening antioxidant activity and identification of active phytochemical compounds of *Scutellariawightiana*Benth.an endemic plant to peninsular India. Res J Biotechnol. 2023;18(5).
44. Ito Y. Golden rules and pitfalls in selecting optimum conditions for high-speed counter-current chromatography. J Chromatograp A. 2005;1065(2):145–68.
45. Sultana N, Ata A, Malik A. A new flavonol glycoside from *Tabernaemontana divaricata* (L.) R Br J Asian Nat Prod Res. 2008;10(6):579–84.
46. Patel JK, Tripathi P, Sharma V, Chauhan NS, Dixit VK. Phospholipase C-γ1 signaling involvement in apoptosis and cell cycle arrest of retinoblastoma cells induced by alcoholic extract of *Tabernaemontana divaricata*. Tumor Biol. 2017;39(7):1010428317719786.
47. Prashant K, Selvakumar S, Singh SK, Singh MM. Antioxidant activity and HPTLC analysis of *Tabernaemontana divaricata (L.)* R Br. J Adv Pharm Technol Res. 2010;1(1):68–74.
48. Deshpande SR, Sathe SS, Salunkhe VR, Vaikos NP, Govindwar SP, Pande VV. Characterization of the major bioactive indole alkaloids from *Tabernaemontana heyneana* wall. Drug Test Anal. 2018;10(9):1441–7.
49. Gobinath P, Packialakshmi P, Vijayakumar K, Abdellattif MH, Shahbaaz M, Idhayadhulla A, et al. Synthesis and cytotoxic activity of novel indole derivatives and their *in silico* screening on spike glycoprotein of SARS-CoV-2. Front Mol Biosci. 2021;8:637989.
50. Parveen N, Khan TH, Ahamad J. Revisiting secondary metabolites from *Tabernaemontana divaricata*: chemical characterization and biological applications. Arabian J Chem. 2019;12(8):4189–99.
51. Rekha S, Vijayan P, Jeya A, Guruvayoorappan C. Bioactive compound apparicine isolated from *Tabernaemontana divaricata* induces G2/M cell cycle arrest and apoptosis in A549 cells through p53-dependent pathway. Environ Toxicol. 2018;33(1):99–113.
52. Yallappa S, Manjappa S, Dhananjaya BL, Vishwanath BS. Synthesis characterization and *in vitro* anticancer evaluation of novel *benzofuran-isatin* derivatives. Bioorg Med Chem Lett. 2016;26(4):1272–6.
53. Vijayakumar R, Arunkumar A, Muthusamy V, Senthilkumar K, Gopinath M, Ramesh Kumar A, et al. Phytochemical analysis and *in vitro* antimicrobial activity of *Tabernaemontana divaricata* (L.) *R.Br. ex Roem*: Schult, Flowers against human pathogens. J Acute Med. 2013;3(1):35–42.
54. Muthukrishnana J, Seifert K, Homannc KH, Lorenz MW. Inhibition of juvenile hormone biosynthesis in *Gryllusbimaculatus*

by *Glycosmis pentaphylla* leaf compounds. Phytochemistry. 1999;50(2):249–54.

55. Chakravarti D, Chakravarti RN, Cohen LA, Dasgupta B, Datta S, Miller HK. Alkaloids of *Glycosmis arborea*—II: structure of arborine. Tetrahedron. 1961;16(1-4):224–50.
56. Paiva SR, Figueiredo MR, Aragão TV, Kaplan MA. Antimicrobial activity *in vitro* of *plumbagin* isolated from *Plumbago* species. Memorias do Instituto Oswaldo Cruz. 2003;98:959–61.
57. Ranjithkumar R, Gokulakrishnan R, Viswanathan V, Sampathkumar P, Yuvarajan R, Rajesh R. Anticancer activity of *Tabernaemontana divaricata* and its bioactive compounds: *in vitro* and *in vivo* studies. Biomed Pharmaco Ther. 2019;109:346–58.
58. Hu Y, Yang W, Han H, Wang P, Zhou Y, Zhang H, et al. The indole alkaloid apparicine induces apoptosis of colon cancer cells via suppression of Akt/NF-κB signaling pathway. Front Pharmacol. 2020;11:241.
59. Kitchen DB, Decornez, H, Furr, JR, Bajorath J. Docking and scoring in virtual screening for drug discovery: methods and applications. Nat Rev Drug Discov. 2004;3(11):935–49.
60. Lot M, Hamblin MR, Rezaei N. COVID-19: transmission, prevention, and potential therapeutic opportunities. Int J Clin Chem Diagnostic Lab Med. 2020;508:254–66.

How to cite this article:
Rajeswari E, Prakash B, Mahendran D, Natarajan D. Anticancer effect of bioactive compound Apparicine isolated from the *Tabernaemontana divaricata* on retinoblastoma cancer cell line (Y^{79}) and *in silico* docking approaches. J App Biol Biotech. 2024;12(6):208-217.
DOI: 10.7324/JABB.2024.175264